

# A bidirectional radio over fiber system with multiband-signal generation using one single-drive MZM

Liang Zhang, Xiaofeng Hu, Pan Cao, Tao Wang, and Yikai Su\*

State Key Lab of Advanced Optical Communication Systems and Networks, Department of Electronic Engineering,  
Shanghai Jiao Tong University, Shanghai, 200240, China

\*yikaisu@sjtu.edu.cn

**Abstract:** We propose and experimentally demonstrate a simple and cost-effective bidirectional radio-over-fiber (RoF) system for transmission of downstream multiband signals and upstream data. At the central station (CS), the multiband data consisting of baseband, micro-wave (MW) and millimeter-wave (MMW) signals are generated using only one single-drive x-cut Mach-Zehnder modulator (MZM), which is driven by a clock signal at radio frequency (RF) port and an electrical data at bias port. Upstream data transmission is realized by re-modulation of filtered frequency-shift-keying (FSK) signal, selected from the multiband signals.

©2011 Optical Society of America

**OCIS codes:** (060.0060) Fiber optics and optical communications; (060.4080) Modulation.

---

## References and links

1. Z. Jia, J. Yu, Y.-T. Hsueh, A. Chowdhury, H.-C. Chien, J. A. Buck, and G.-K. Chang, "Multiband signal generation and dispersion-tolerant transmission based on photonic frequency tripling technology for 60-GHz radio-over-fiber systems," *IEEE Photon. Technol. Lett.* **20**(17), 1470–1472 (2008).
  2. J. Yao, "Microwave Photonics," *J. Lightwave Technol.* **27**(3), 314–335 (2009).
  3. A. Martinez, V. Polo, and J. Marti, "Simultaneous baseband and RF optical modulation scheme for feeding wireless and wireline heterogeneous access network," *IEEE Trans. Microw. Theory Tech.* **49**(10), 2018–2024 (2001).
  4. G. Yoffe, R. Waterhouse, D. Novak, A. Nirmalathas, and C. Lim, "Millimeter-Wave broad-band fiber-wireless system incorporating baseband data transmission over fiber and remote LO delivery," *J. Lightwave Technol.* **18**(10), 1355–1363 (2000).
  5. C. Lin, J. Chen, P. Peng, C. Peng, W. Peng, B. Chiou, and S. Chi, "Hybrid optical access network integrating fiber-to-the-home and radio-over-fiber systems," *IEEE Photon. Technol. Lett.* **19**(8), 610–612 (2007).
  6. M. Bakaul, A. Nirmalathas, C. Lim, D. Novak, and R. Waterhouse, "Hybrid multiplexing of multi-band optical access technologies towards an integrated DWDM network," *IEEE Photon. Technol. Lett.* **18**(21), 2311–2313 (2006).
  7. Q. Chang, H. Fu, and Y. Su, "Simultaneous Generation and Transmission of Downstream Multi-band Signals and Upstream Data in a Bidirectional Radio over Fiber System," *IEEE Photon. Technol. Lett.* **20**(3), 181–183 (2008).
  8. Y. Hsueh, Z. Jia, H. Chien, J. Yu, and G. Chang, "A Novel Bidirectional 60-GHz Radio-Over-Fiber Scheme With Multiband Signal Generation Using a Single Intensity Modulator," *IEEE Photon. Technol. Lett.* **21**(18), 1338–1340 (2009).
  9. K. Ikeda, T. Kuri, and K. Kitayama, "Simultaneous three-band modulation and fiber-optic transmission of 2.5-Gb/s baseband, microwave-, and 60-GHz-band signals on a single wavelength," *J. Lightwave Technol.* **21**(12), 3194–3202 (2003).
  10. L. Zhang, X. Hu, P. Cao, T. Wang, and Y. Su, "A Multiband Radio over Fiber System Using a Single-drive Mach-Zehnder Modulator," in *Proceeding of ACP 2010*, FP5.
  11. Q. Chang, Y. Tian, J. Gao, T. Ye, Q. Li, and Y. Su, "Generation and Transmission of Optical Carrier Suppressed-Optical Differential (Quadrature) Phase-Shift Keying (OCS-OD(Q)PSK) Signals in Radio Over Fiber Systems," *J. Lightwave Technol.* **26**(15), 2611–2618 (2008).
  12. J. Yu, Z. Jia, L. Yi, Y. Su, G. K. Chang, and T. Wang, "Optical millimetre wave generation or up-conversion using external modulators," *IEEE Photon. Technol. Lett.* **18**(1), 265–267 (2006).
-

## 1. Introduction

The next-generation access networks are converging wireline and wireless services to offer end users more choices and greater convenience. It is desirable to develop a radio-over-fiber (RoF) system to serve both fixed and mobile customers with high capacity, large bandwidth and increased mobility in a cost-effective way [1–5]. Among them, multiband optical transmission technology, which can simultaneously deliver baseband, micro-wave (MW) and millimeter-wave (MMW) signals, is an attractive candidate. It enables flexible applications in future access networks, where wireline data transports and wireless signal deliveries at different radio frequency (RF) carriers are seamlessly converged in an integrated platform. Recently, some demonstrations on simultaneous transmission of multiband data were performed [6–9]. However, individual light sources and modulators were needed to generate multiband signals [6], which increase the system complexity and the configuration cost. Ref [7], demonstrated a RoF system for generation of multiband signals using a dual-parallel Mach-Zehnder modulator (DPMZM) followed by a single-drive Mach-Zehnder modulator (MZM), with complex transmitter architecture and high insertion loss. Multiband signals were obtained using a dual-arm MZM driven by a 20-GHz clock in one arm and a 40-GHz electrical sub-carriers multiplexing (SCM) signal in the other arm, which required high-frequency synthesizer and high-speed electrical devices such as quadruplers and mixers [8]. In Ref [9], an electro-absorption modulator (EAM) was employed to generate multiband signals, where many electrical devices were needed.

Recently, we reported a cost-effective method to produce multiband signals utilizing a single-drive x-cut MZM [10]. Here we describe the detailed principle, and provide experimental results and their discussions. The transmitter in the central station (CS) consists of only a single-drive x-cut MZM without additional RF electronic processing devices (combiners or mixers), enabling a low-cost architecture. To the best of our knowledge, this is the first time that baseband, 20-GHz MW and 40-GHz MMW signals are simultaneously generated using only a 10-GHz single-drive x-cut MZM. At the base station (BS), uplink data is re-modulated on the downlink signals, eliminating additional light sources and complicated wavelength management. In addition, our scheme is also scalable to achieve above 100-GHz MMW.

## 2. Principle

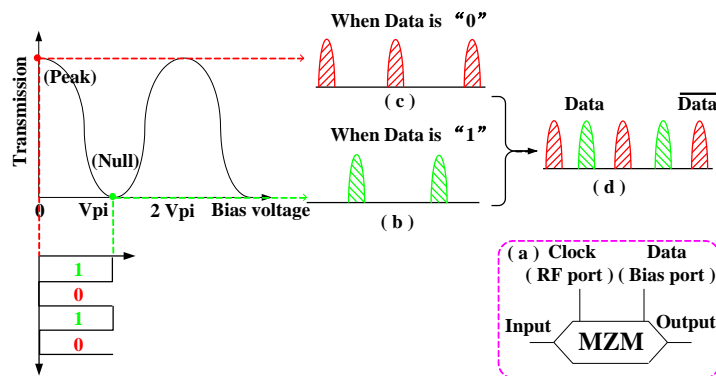


Fig. 1. Principle of the generation of multiband signals.

Figure 1 shows the principle of generation of multiband signals based on a single-drive x-cut MZM, which is driven by a clock signal at the RF port and a unipolar Data source at the bias port (Fig. 1 (a)). The clock signal is  $S_{RF} = \alpha V_{\pi} \cos(\omega_{RF} + \theta)$ , and the Data is  $S_D = V_{\pi} \varepsilon(t)$ , where  $V_{\pi}$  is the half-wave voltage of the MZM, and  $\alpha$  is amplitude of the clock signal normalized to the half-wave voltage,  $\omega_{RF}$  and  $\theta$  are the angle frequency and phase of the clock signal,

respectively, and  $\varepsilon(t) = 0$  or 1, depending on the Data. According to Ref [11], the output field of the MZM can be expressed by:

$$\begin{aligned}
E_{out} = & E_0 J_0\left(\frac{\pi}{2}\alpha\right) \cos\left[\frac{\pi}{2}\varepsilon(t)\right] \cos(\omega_c t + \theta_0) \\
& + E_0 J_1\left(\frac{\pi}{2}\alpha\right) \sin\left[\frac{\pi}{2}\varepsilon(t)\right] \cos[(\omega_c \pm \omega_{RF})t + \theta_0 \pm \theta] \\
& + E_0 J_2\left(\frac{\pi}{2}\alpha\right) \cos\left[\frac{\pi}{2}\varepsilon(t)\right] \cos[(\omega_c \pm 2\omega_{RF})t + \phi_0 \pm 2\theta],
\end{aligned} \tag{1}$$

where  $E_0$ ,  $\omega_c$  and  $\theta_0$  are the amplitude, angle frequency and phase of the input optical signal, respectively. In Eq. (1), only the baseband, the first-order and the second-order sidebands are considered, while the high-order components are ignored due to the negligible optical power.

When  $\varepsilon(t)$  is “1” (high electrical level), and the MZM is biased at its transmission null, the even-order harmonics are suppressed and an optical carrier suppression (OCS) signal (Fig. 1 (b)) is generated, which can be expressed by:

$$E_{out1} = E_0 J_1\left(\frac{\pi}{2}\alpha\right) \sin\left[\frac{\pi}{2}\varepsilon(t)\right] \cos[(\omega_c \pm \omega_{RF})t + \theta_0 \pm \theta]. \tag{2}$$

While, when  $\varepsilon(t)$  is “0” (low electrical level), the MZM is biased at the peak of the transmission curve and the output signal consists of the optical carrier and second-order harmonic components (Fig. 1 (c)), which can be given by:

$$\begin{aligned}
E_{out2} = & E_0 J_0\left(\frac{\pi}{2}\alpha\right) \cos\left[\frac{\pi}{2}\varepsilon(t)\right] \cos(\omega_c t + \theta_0) \\
& + E_0 J_2\left(\frac{\pi}{2}\alpha\right) \cos\left[\frac{\pi}{2}\varepsilon(t)\right] \cos[(\omega_c \pm 2\omega_{RF})t + \theta_0 \pm 2\theta].
\end{aligned} \tag{3}$$

As a result, if the electrical level of the Data switches between the high and low levels, a five-tone signal (Fig. 1 (d)), consisting of baseband and MMW signals carrying inversed Data, and MW signal carrying the Data, can be achieved. By properly adjusting the amplitude of the clock signal and the level of the Data signal, the five-tone signal could have the same optical power in each band. Since the transmitted information is carried on the amplitudes of the multiband optical carriers, which are controlled by the levels of Data signal at the bias port of MZM, the modulation format should only be on-off keying (OOK) signal. However, for the low-cost RoF optical access network, OOK modulation format maybe more attractive due to simple modulation and demodulation technologies.

The schematic diagram of the proposed bidirectional RoF system is illustrated in Fig. 2. A continuous wave (CW) light is launched into a commercial single-drive x-cut MZM, which is modulated to simultaneously generate baseband, MW and MMW signals. After the transmission, an optical filter is used to separate each band at the BS. A low-speed photodetector (PD) is employed to receive the baseband signal and two high-speed PDs are utilized to recover the MW and MMW signals. Thus the proposed scheme provides wireline and two wireless signals for the end users. In order to save light sources at the BS, we use a band-pass filter to select the baseband and the right band of the MW signal, and generate a frequency-shift-keying (FSK) signal, which is then OOK re-modulated by upstream data. The upstream signal is sent back to the CS, where it is detected by a low-speed receiver. Using this design, one can simultaneously deliver downstream multiband signals and upstream data with a single wavelength in a bidirectional RoF system.

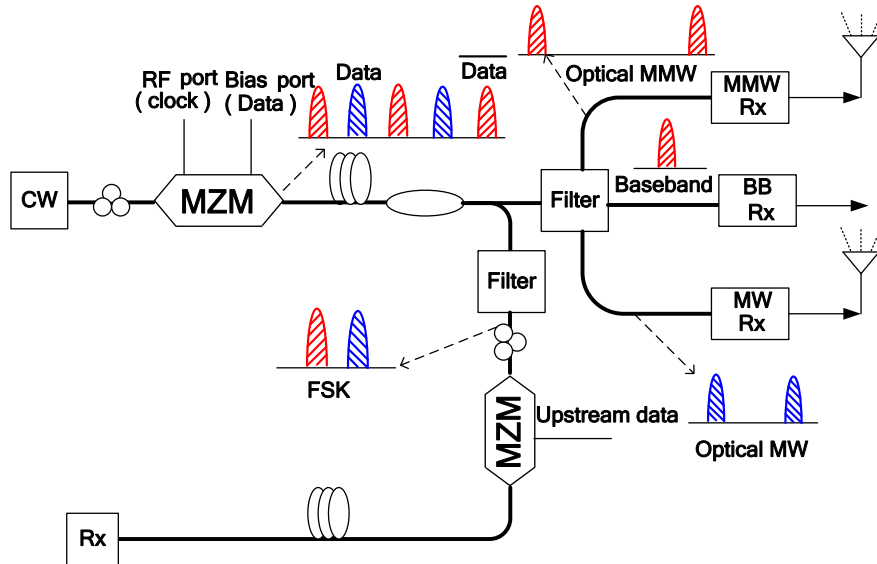


Fig. 2. Schematic diagram of the proposed RoF system.

### 3. Experimental setup and results

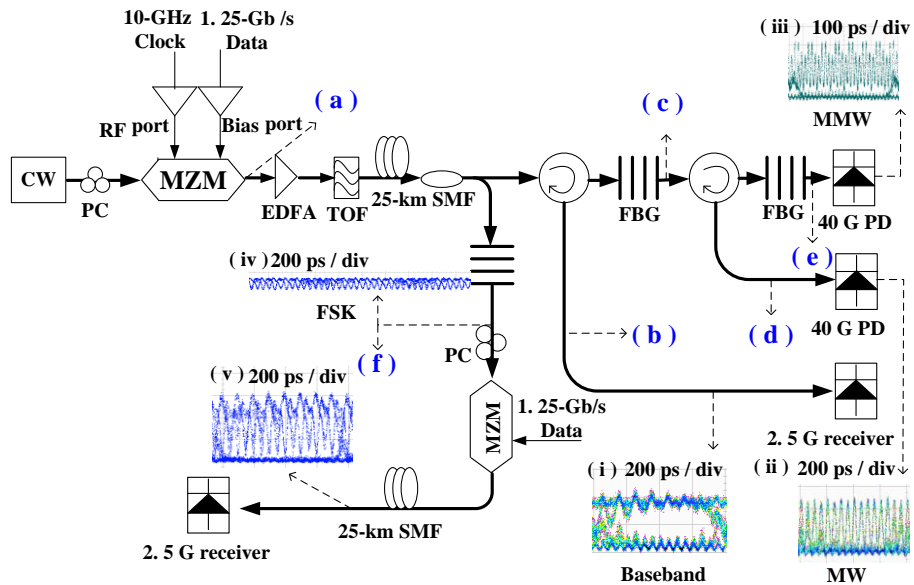


Fig. 3. Experimental setup of the proposed bidirectional RoF system. (i) Optical eye diagram of baseband signal, (ii) electrical eye diagram of MW signal, (iii) electrical eye diagram of MMW signal, (iv) optical eye diagram of FSK signal, (v) optical eye diagram of re-modulated ASK signal. (a) - (f) correspond to the optical spectra shown in the Fig. 4.

To verify the proposed scheme, we perform an experiment with the setup depicted in Fig. 3. At the CS, a CW light from a tunable laser (Santec TSL-210F) at 1550.99 nm is injected into a polarization controller (PC) and then fed into a 10-GHz single-drive x-cut MZM (JDSU OC-192) with a half-wave voltage of 5.5 V. The MZM is driven by an amplified 10-GHz clock with a peak-to-peak voltage of 12.7 V at the RF port. The RF modulation index is  $\sim 1.81$ . Although the nonlinearity induced by the higher RF modulation index could generate some

unwanted higher-order sidebands, these tones have much lower powers. In addition, optical filter can further suppress those unwanted components. The output of the MZM (Fig. 4(a)), consisting of baseband, 20-GHz MW and 40-GHz MMW, is amplified to reach a power level of 6 dBm using an erbium-doped fiber amplifier (EDFA). Then a tunable optical filter (TOF) with a 3-dB bandwidth of 1.6 nm is employed to suppress amplified spontaneous emission (ASE) noise.

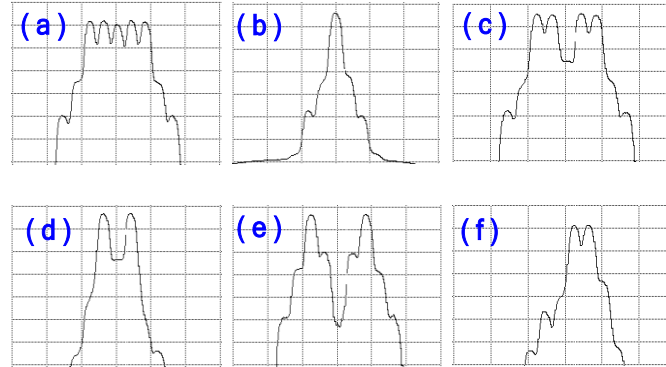


Fig. 4. Optical spectra taken at different positions as indicated in Fig. 3. Spectral resolution: 0.07 nm. X-axis: 0.2 nm/div; Y-axis: 5 dB/div. (a) Multiband signals, (b) reflected baseband signal, (c) passing signal from the first FBG, (d) reflected MW signal, (e) passing MMW signal, (f) filtered FSK signal.

After transmission of 25-km standard single-mode fiber (SMF), at the BS, the signal is separated by a fiber Bragg grating (FBG) with a 3-dB bandwidth of 0.106 nm and a reflection ratio of 90%. The baseband signal is reflected and its optical spectrum and optical eye diagram are shown in Fig. 4 (b) and inset (i) of Fig. 3, respectively. The passing signals are injected into a second FBG with a 3-dB bandwidth of 0.203 nm and a reflection ratio of 96% to separate the MW and MMW signals, whose optical spectra are provided in Fig. 4 (d) and (e), respectively. A 40-GHz PD is used to receive the MW and MMW signals and their electrical eye diagrams are shown in insets (ii) and (iii) of Fig. 3, respectively. For bit-error-rate (BER) measurements, 2.5-GHz receivers are used to detect the MW and MMW signals due to the lack of high-speed mixers, similar results could be found regardless of the detection methods [11,12]. A part of the multiband signal is tapped by a 50:50 optical coupler and filtered by an FBG to generate a FSK signal with the same optical power in both selected components, whose optical spectrum and optical eye diagram are provided in Fig. 4 (f) and inset (iv) of Fig. 3. After passing through a PC, the generated FSK signal is OOK re-modulated using a MZM driven by a 1.25-Gbps upstream data with a PRBS length of  $2^{31}-1$ . The optical eye diagram of the FSK/OOK orthogonal modulation signal is shown in inset (v) of Fig. 3. After transmission through 25-km SMF, at the CS, the upstream data is detected by a 2.5-GHz receiver. We compare the BER performance of FSK/IM re-modulation with that of intensity modulation on a CW light by VPI simulation software. The difference in power penalties is  $\sim 0.5$  dB. The polarization controller (PC) in the BS is used to maintain good transmission performance, which can be eliminated if using commercially available polarization-insensitive modulators. In our experiment, a temperature controller (E-TEK MLDC-1016) is used to keep the temperature stable for FBGs.

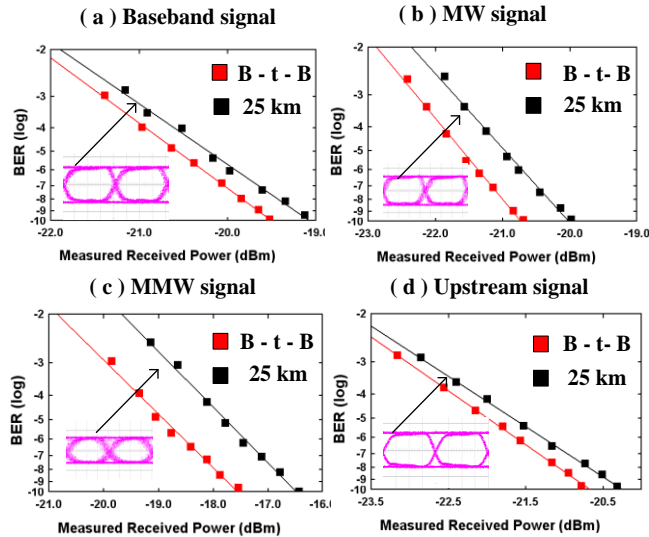


Fig. 5. BER curves and electrical eye diagrams after 25-km SMF transmission. (a) Downstream baseband signal, (b) downstream MW signal, (c) downstream MMW signal, (d) upstream re-modulation signal.

The BER performances and electrical eye diagrams of the downstream multiband signals and upstream data are provided in Fig. 5. For the baseband signal, the power penalty is  $\sim 0.3$  dB after transmission of 25-km SMF. Error-free performances are obtained for both MW and MMW signals with  $\sim 1.2$ -dB power penalties, which can be attributed to chromatic dispersion (CD) and non-ideal filtering effect. The degradation of the BER performance for the baseband signal is caused by the residual MW components. The MMW signal is also affected greatly by the MW components with only 8-dB suppression ratio, which may result in low BER performance. Better BER performances can be achieved for the signals if FBGs with good performances are available. We also measure the BER of the upstream data, whose power penalty is about 0.4 dB. The electrical eye diagrams of the multiband signals and upstream data are provided in insets of Fig. 5.

#### 4. Conclusion

We have proposed a simple, cost-effective, and scalable RoF architecture, and experimentally demonstrated simultaneous generation and transmission of the 1.25-Gbps downstream baseband, 20-GHz MW and 40-GHz MMW signals using only one single-drive x-cut MZM, with symmetric upstream data transmission over 25-km SMF. Error-free performances are achieved for all the data with less than 1.2-dB power penalties. The experiments verify that our scheme could be a desirable candidate for future wireline and wireless converged networks.

#### Acknowledgement

This work was supported by the 863 High-Tech Program (2009AA01Z257).